

Tissue-specific Short Chain Fatty Acid Metabolism and Slow Metabolic Recovery after Ischemia from Hyperpolarized NMR *in Vivo*^{*[5]}

Received for publication, September 15, 2009, and in revised form, October 22, 2009. Published, JBC Papers in Press, October 27, 2009, DOI 10.1074/jbc.M109.066407

Pernille R. Jensen[‡], Torben Peitersen[‡], Magnus Karlsson[‡], René in 't Zandt[‡], Anna Gisselsson[‡], Georg Hansson[‡], Sebastian Meier[§], and Mathilde H. Lerche^{‡1}

From [‡]Imagnia AB, 200 41 Malmö, Sweden and the [§]Carlsberg Laboratory, Gamle Carlsberg Vej 10, 2500 Valby, Denmark

Mechanistic details of mammalian metabolism *in vivo* and dynamic metabolic changes in intact organisms are difficult to monitor because of the lack of spatial, chemical, or temporal resolution when applying traditional analytical tools. These limitations can be addressed by sensitivity enhancement technology for fast *in vivo* NMR assays of enzymatic fluxes in tissues of interest. We apply this methodology to characterize organ-specific short chain fatty acid metabolism and the changes of carnitine and coenzyme A pools in ischemia reperfusion. This is achieved by assaying acetyl-CoA synthetase and acetyl-carnitine transferase catalyzed transformations *in vivo*. The fast and predominant flux of acetate and propionate signal into acyl-carnitine pools shows the efficient buffering of free CoA levels. Sizeable acetyl-carnitine formation from exogenous acetate is even found in liver, where acetyl-CoA synthetase and acetyl-carnitine transferase activities have been assumed sequestered in different compartments. *In vivo* assays of altered acetate metabolism were applied to characterize pathological changes of acetate metabolism upon ischemia. Coenzyme pools in ischemic skeletal muscle are reduced *in vivo* even 1 h after disturbing muscle perfusion. Impaired mitochondrial metabolism and slow restoration of free CoA are corroborated by assays employing fumarate to show persistently reduced tricarboxylic acid (TCA) cycle activity upon ischemia. In the same animal model, anaerobic metabolism of pyruvate and tissue perfusion normalize faster than mitochondrial bioenergetics.

Acetyl coenzyme A (acetyl-CoA)² is a central metabolite that connects metabolic paths such as fatty acid degradation and synthesis, cholesterol biosynthesis, glycolysis, and the TCA cycle (Fig. 1). Thus, acetyl-CoA is among the key molecules of energy and intermediary metabolism. Acetyl-CoA is generated

by a number of enzymes in mammals including pyruvate dehydrogenase, β -ketothiolase, and ATP citrate-lyase (1). A less well-explored metabolic pathway forming acetyl-CoA in mammals is the acetyl-CoA synthetase (AceCS)-catalyzed catabolism of acetate (Fig. 1), which accounts for up to 10% of the energy expenditure in humans (2).

Esterification of carboxylic acids is a common means of generating activated molecules for entrance into metabolic pathways and renders the CoA-activated metabolite largely membrane impermeable. Pools of acyl-CoA esters in different cellular compartments require tight regulation because of their metabolic activity and because of the signaling function of some CoA esters (3). Under normal conditions, free CoA is regenerated by the metabolism esters, whereas large amounts of CoA esters may accumulate under stress conditions (4). Sufficient pools of free CoA are ensured under these conditions by buffering acyl-CoA:CoA ratios through transesterifications of acyl-CoA with carnitine. Carnitine also provides a shuttle for the flux of CoA-activated metabolites between intracellular compartments (5). Transesterification between CoA and carnitine esters by carnitine acyltransferases is freely reversible and thus occurs without wasting free energy on hydrolysis and resynthesis of the esters. The short fatty-acid specific carnitine acetyltransferase CrAT ensures compartmental buffering of CoA and acetyl-CoA pools in mitochondria, endoplasmic reticulum, and peroxisomes (3, 6).

The overall importance of the carnitine system is evidenced by the severe clinical manifestations of primary genetic carnitine deficiency diseases leading to myopathies, heart attacks, and death (4, 7, 8). Metabolic disturbance of the carnitine/CoA system occurs among others secondary to ischemia and hypoxia, cardiac failure, fatty acid oxidation disorders, ketosis, and diabetes (3, 4, 9). This suggests assaying metabolism of exogenous acetate or propionate by AceCS and CrAT (Fig. 1) *in vivo* for detection of pathological CoA and carnitine levels.

The precise physiological role of mammalian acetate metabolism has remained elusive and has attracted renewed interest, as mammalian acetate metabolism is modulated by sirtuins implicated in organism longevity (10, 11). Functional *in vivo* data on tissue acetate metabolism is required because of shortcomings in extrapolating *in vitro* and *ex vivo* data on pathway regulation to physiological settings. Previous use of acetate tracers *in vivo* has assessed oxidative tissue metabolism by NMR isotopomer analysis of steady-state ¹³C

* This work was supported by a commercial research grant from GE HealthCare.

[5] The on-line version of this article (available at <http://www.jbc.org>) contains supplemental "Methods" and Fig. S1.

¹ To whom correspondence should be addressed: Imagnia AB, Box 8225, 200 41 Malmö, Sweden. Tel.: 46-40-82760; Fax: 46-40-82761; E-mail: mathilde.lerche@imagnia.se.

² The abbreviations used are: acetyl-CoA, acetyl coenzyme A; AceCS, acetyl-CoA synthetase; CrAT, carnitine acetyltransferase; DNP, dynamic nuclear polarization; ECG, electrocardiogram; MR, magnetic resonance; MRS, magnetic resonance spectroscopy; NMR, nuclear magnetic resonance; OX063, Tris(8-carboxy-2,2,6,6-(tetra(hydroxyethyl)-benzo-[1,2,4,5']-bis-(1,3)-dithiole-4-yl)-methyl sodium salt; TCA cycle, tricarboxylic acid cycle; GFP, green fluorescent protein.

In Vivo Assays of Slow Metabolic Recovery

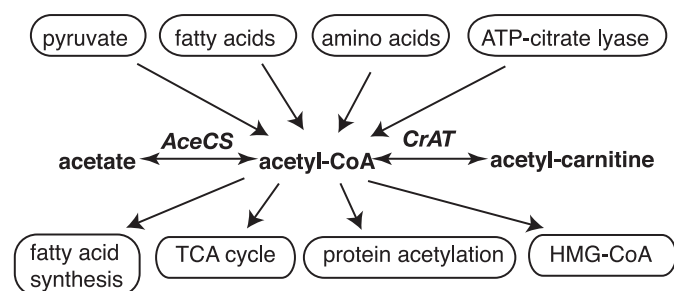


FIGURE 1. **Simplified account of the main metabolic routes involving acetyl-CoA.** Acetyl-CoA formation from exogenous acetate is catalyzed by acetyl-CoA synthetase (AceCS), whereas carnitine acetyltransferase (CrAT) regenerates free CoA and forms acetyl-carnitine.

incorporation into metabolites and by radiolabel assays of acetate uptake and clearance (12–21). These approaches are limited in temporal and spatial resolution, in their use under non-steady-state conditions (22) or in the lack of chemical detail provided. Instantaneous measurements of metabolic pathway activity *in vivo* or in perfused organs have become feasible with polarization enhanced (*i.e.* hyperpolarized) NMR tracers (23), but have largely been limited to the use of pyruvate (24–33).

Here, we report *in vivo* measurements of acetate metabolism by AceCS and CrAT (Fig. 1) to gain insight (i) on the capacity of different organs in healthy metabolic states to catabolize acetate and (ii) on alterations in acetate metabolism secondary to energy imbalance and altered CoA and carnitine pools upon muscle ischemia. We find that [$1\text{-}^{13}\text{C}$]acetate, [$1\text{-}^{13}\text{C}$]acetyl-CoA, and [$1\text{-}^{13}\text{C}$]acetyl-carnitine signals in myocardium reflect high reliance on fatty acid metabolism under normoxic conditions and the capacity to feed acetate into the TCA cycle. Unexpectedly, sizeable flux of exogenous acetate to acetyl-carnitine is also detected in liver, where cytosolic AceCS and non-cytosolic CrAT activity have been assumed spatially sequestered (3, 34). Upon skeletal muscle ischemia, strongly reduced flux through the AceCS and CrAT catalyzed reactions indicates reduced CoA and carnitine pools even 1 h after ischemia has been released. Use of hyperpolarized [$1\text{-}^{13}\text{C}$]pyruvate on the other hand shows that increased lactate signal caused by anaerobic glycolysis under conditions of high [NADH]:[NAD $^+$] and pyruvate dehydrogenase inhibition normalizes substantially faster than acetate metabolism. These findings point toward kinetic selection against acetate metabolism during recovery because of the high K_m value of AceCS for CoA (17). Persistently impaired mitochondrial bioenergetics in ischemia reperfusion is supported by use of hyperpolarized [$1,4\text{-}^{13}\text{C}_2$]fumarate to assay inhibition of TCA cycle enzymes *in vivo*.

EXPERIMENTAL PROCEDURES

Materials—Sodium [$1\text{-}^{13}\text{C}$]acetate, [$1\text{-}^{13}\text{C}_1$]acetic acid, and sodium [$1\text{-}^{13}\text{C}$]propionate were obtained from Cambridge Isotope Laboratories. GE Healthcare provided [$1\text{-}^{13}\text{C}$]pyruvic acid, and trityl radical OX063 (Tris(8-carboxy-2,2,6,6-(tetra-(hydroxyethyl)-benzo-[1,2-4,5']-bis-(1,3)-dithiole-4-yl)-methyl sodium salt) and AH111501 (Tris(8-carboxy-2,2,6,6-(tetra(methoxyethyl) benzo-[1,2-4,5']-bis-(1,3)-dithiole-4-

yl)methyl sodium salt). The gadolinium complex 3-Gd (1,3,5-tris-(*N*-(DO3A-acetamido)-*N*-methyl-4-amino-2-methylphenyl)-[1,3,5]triazine-2,4,6-trione) was synthesized in house. All other chemicals were obtained from Sigma Aldrich. Inbred laboratory mice of strain C57BL/6 were obtained from Charles River Laboratories International and given free access to standard mice chow and water.

Preparation and Hyperpolarization of ^{13}C -labeled Substances—Acetate was prepared for hyperpolarization as previously described (35). A detailed optimization protocol is given in the [supplemental Methods](#). For propionate preparation, the same protocol was used as for acetate. Pyruvic acid was prepared by adding 24.8 mg trityl radical OX063 and 1.1 mg of Gd complex to 1035 mg [$1\text{-}^{13}\text{C}$]pyruvic acid, which results in a [$1\text{-}^{13}\text{C}$]pyruvic acid preparation containing 15 mM OX063 and 0.5 mM Gd complex. [$1,4\text{-}^{13}\text{C}_2$]Fumaric acid was prepared by dissolving 40 mg (0.34 mmol) in 72 mg of a DMSO solution containing 19 mM AH111501 and 0.8 mM Gd complex.

DNP preparations were hyperpolarized in a polarizer as described by Ardenkjær-Larsen *et al.* (23). The hyperpolarized sample was subsequently dissolved in a phosphate buffer (40 mM, osmolality adjusted with NaCl to 210 mOsm) to provide a 50 mM solution of hyperpolarized substance at at pH of 7.1 ± 0.1 , an osmolality of 274 ± 8 mOsm and a polarization of $17 \pm 1\%$ for acetate, $22 \pm 1\%$ for propionate, $23 \pm 2\%$ for pyruvate and $30 \pm 2\%$ for fumarate during the administration. In the dissolution buffer of pyruvic acid and fumaric acid equivalent amounts of NaOH were added to neutralize the acids. A dose of 0.44 mmol/kg was infused during 6 s resulting in an approximate blood concentration of 5 mM tracer.

^{13}C MRS *in Vivo*—A catheter was placed in the tail vein, and animals were positioned in a 2.35 T Bruker Biospec Avance II MR scanner. Anesthesia was maintained in the MR system by a gas mixture of oxygen and nitrous oxide with 2% isoflurane. Gas flow was 200 ml/min O $_2$ and 200 ml/min N $_2$ O. Body temperature of the animals was controlled to vary within 37.0 ± 0.2 °C. ECG, breathing, and rectal temperature were all monitored with a S. A. Instrument 1025 MR compatible animal monitoring system. Injection of the substances did not lead to abnormal effects on the physiological parameters that were monitored.

MR imaging was performed using a dual-tuned $^1\text{H}\text{-}^{13}\text{C}$ birdcage resonator with inner diameter of 72 mm and a standard proton MR imaging sequence to retrieve anatomic information. ^{13}C spectra of myocardial and liver metabolism were acquired with a 12-mm ^{13}C surface coil placed on the sternum or abdomen of the mouse, respectively. Spectra in myocardium and liver were recorded either with a 90° flip angle 15 s after the start of the injection or with a time series of 30 one-dimensional spectra obtained with 30° flip angles and a repetition time of 3 s. For the ischemic model, an 8-mm ^{13}C surface coil was placed around the hind leg of the mouse, and a time series of 30 one-dimensional spectra was obtained with 25° flip angles and a repetition time of 4 s for acetate and pyruvate injections. Spectra of fumarate injections were recorded with a time series of 60 one-dimensional spectra obtained with 10° flip angles and a repetition time of 2 s.

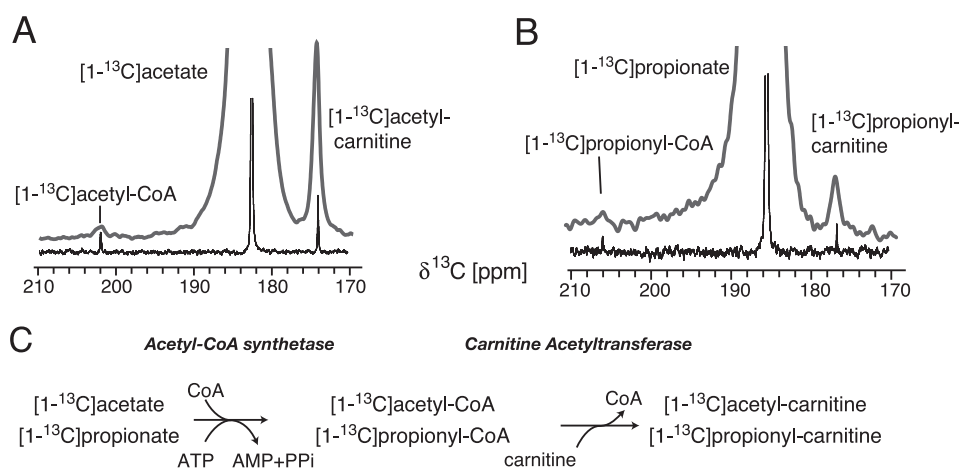


FIGURE 2. *In vivo* and *in vitro* metabolism of hyperpolarized $[1-^{13}\text{C}]$ acetate and $[1-^{13}\text{C}]$ propionate (A and B). *In vivo* NMR spectra (bold gray lines) of myocardium are recorded with a 90° flip angle pulse after injecting $175\text{-}\mu\text{l}$ hyperpolarized substrate. Spectra of reactions conducted with 2 mM hyperpolarized substrate and isolated AceCS and CrAT *in vitro* according to the scheme in C are shown as thin black lines. Identity of *in vivo* metabolite signals with acyl-CoA and acyl-carnitine adducts is validated by spectral frequencies *in vivo* for both substrates.

Ischemia—Hindlimb ischemia was introduced by occlusion with a string for 30 min as described by in 't Zandt *et al.* (36). Occlusion was performed at a constant force for 30 min and was released 5 min before injection of ^{13}C -labeled substrate. After data acquisition, the mouse was kept in the scanner for further 55 min before a second injection of ^{13}C -labeled substrate. Data were analyzed in Jmru (37). Eight spectra were summed starting from the first spectrum where the acetate peak appears. Sum spectra were then analyzed in batch. The same methodology was applied for pyruvate metabolism. Fumarase activities were indexed by signal area ratios of malate and fumarate 22 s after fumarate injection.

^{13}C DNP Enzymatic Assays—5-mm NMR tubes were prepared with 4.7 units/ml acetyl-CoA synthetase, 125 units/ml carnitine acetyltransferase, 6 mM coenzyme A, 10 mM carnitine, 10 mM ATP, 75 mM Tris buffer of pH 7.6, 7.5 mM MgCl_2 , and 2 mM dithiothreitol for enzymatic *in vitro* DNP assays (35). The assay mixture was kept at 37°C in a water bath for 15 min prior to experiments. Hyperpolarized short chain fatty acid ($[1-^{13}\text{C}]$ acetate or $[1-^{13}\text{C}]$ propionate) was added to a final concentration of 2 mM. Real-time reaction kinetics was followed by acquiring low flip angle (10°) ^{13}C NMR spectra every 2 s. *In vitro* assays were performed on a 400 MHz Varian Inova spectrometer.

RESULTS

Fast Activation of Acetate to Esters—*In vivo* NMR spectra of acetate metabolism were recorded in mouse heart, liver, and skeletal muscle supplied with hyperpolarized $[1-^{13}\text{C}]$ acetate. Hyperpolarized *in vivo* NMR provides sufficient sensitivity to detect conversion of the marker to different molecular species. In the case of acetate, two metabolites were detected at 202.1 ppm and 174 ppm in the heart (Fig. 2A) in addition to the dominating substrate signal (at 182.6 ppm). Signal assignments to acetyl-CoA (202.1 ppm) and acetyl-carnitine (174 ppm) were supported *in vitro* in a reaction with purified AceCS and CrAT, which yields acetyl-CoA and acetyl-carnitine NMR signals at the spectral positions detected *in vivo* (Fig. 2, A and C).

Metabolism of Exogenous Propionate—AceCS and CrAT activity *in vivo* and *in vitro* were additionally assessed by the use of hyperpolarized $[1-^{13}\text{C}]$ propionate, which also is a substrate for AceCS (38) and CrAT (5) catalyzed reactions. As in the case of hyperpolarized $[1-^{13}\text{C}]$ acetate, two reaction products can be detected *in vivo* (206.1 and 176.9 ppm, Fig. 2B), which can be ascribed to CoA and carnitine esters of propionate in an *in vitro* reaction with purified AceCS and CrAT (Fig. 2, B and C).

Propionate is found to be a substrate for short chain fatty acid metabolism *in vivo* in agreement with reports of similar activities and Michaelis constants of CrAT

toward acetyl-CoA and propionyl-CoA *in vitro* (39, 40). Lower substrate preference of AceCS for propionate is reflected by lower intensities of $[1-^{13}\text{C}]$ propionyl-CoA and $[1-^{13}\text{C}]$ propionyl-carnitine signals as compared with respective acetyl esters in DNP-NMR assays *in vivo* (Fig. 2). This finding is in agreement with *in vitro* data indicating that propionate is a less preferred substrate of AceCS than acetate (38).

Tissue Differences of Acetate Activation—Acetate was accordingly employed as the *in vivo* biomarker of choice for assaying short chain fatty acid metabolism in different organs and in ischemic tissue. A time series showing myocardial metabolism of hyperpolarized $[1-^{13}\text{C}]$ acetate *in vivo* is given in Fig. 3. Signal build-up or decay because of chemical transformation is convoluted with signal decay due to relaxation of the hyperpolarized spin ensemble. Maximum $[1-^{13}\text{C}]$ acetyl-carnitine signal in the dynamic series was used to define the time after infusion, where metabolism of hyperpolarized $[1-^{13}\text{C}]$ acetate is most sensitively detected. Metabolic differences of liver and myocardium in living animals can be assessed from the obtained hyperpolarized NMR spectra, which show a ~ 3 -fold higher acetyl-carnitine:acetyl-CoA signal ratio in myocardium than in liver. Notwithstanding, both acetyl-carnitine and acetyl-CoA signal can be detected in liver (Fig. 3, C and D).

Acetate Metabolism in Ischemia-Reperfusion—Pathology-related changes to the cellular metabolism were assessed in skeletal muscle by the use of hyperpolarized $[1-^{13}\text{C}]$ acetate. A well-characterized model of skeletal muscle ischemia was employed, where ischemia is induced by occluding blood flow in hindlimb skeletal muscle. This model has previously been characterized by *in vivo* ^{31}P NMR, which shows recovery of phosphocreatine to $\sim 90\%$ of preischemic values within 16 min after occluding blood flow for 30 min, while ATP signal is only weakly reduced during ischemia because of the regeneration of ATP from phosphocreatine (36). Metabolic pathway activities were assayed in this model by $[^{13}\text{C}]$ DNP-NMR experiments performed before occlusion of blood flow for 30 min (control), after 5 min of reperfusion and after 1 h of reperfusion. Resultant spectra show a reduction of acetyl-carnitine formation from exogenous ace-

In Vivo Assays of Slow Metabolic Recovery

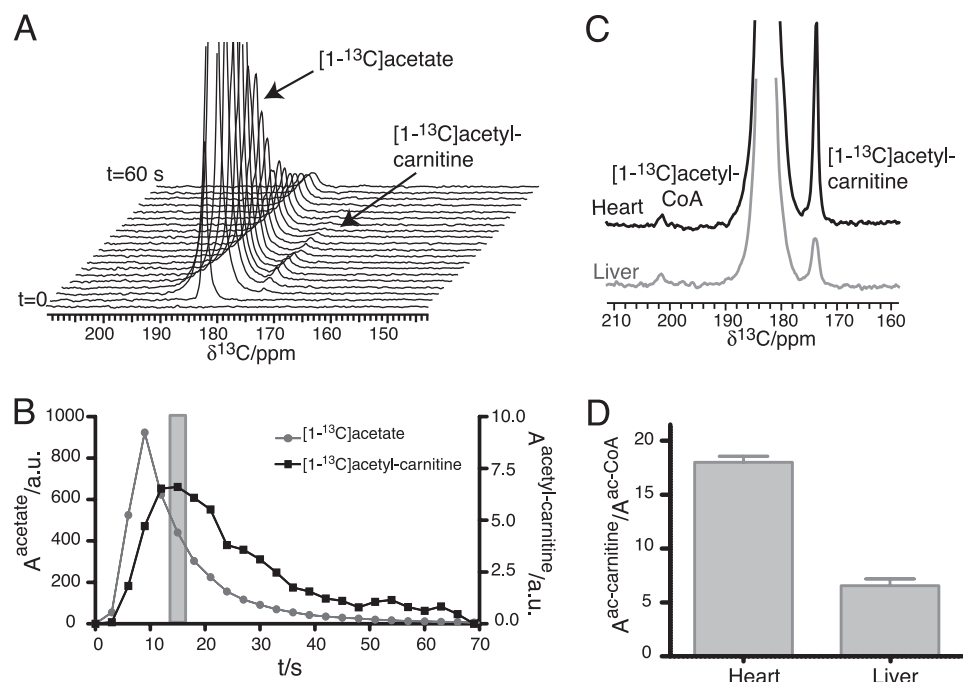


FIGURE 3. Signal intensities of acetate and acetyl-carnitine in myocardium. A time series of spectra was recorded by applying a 30° flip angle pulse every 3 s (A). Signal intensities reflect chemical transformation and relaxation of the hyperpolarized spin ensemble. Acetyl-carnitine and acetyl-CoA signals were measured in heart and liver with single 90° flip angle pulses after 15 s, where maximum acetyl-carnitine signal is observed in the time series (B). C and D, different ratios of acetyl-carnitine and acetyl-CoA signal directly indicate different acetate metabolism in liver and heart ($p < 0.01$; $n = 6$). Data values are displayed as mean \pm S.D. throughout.

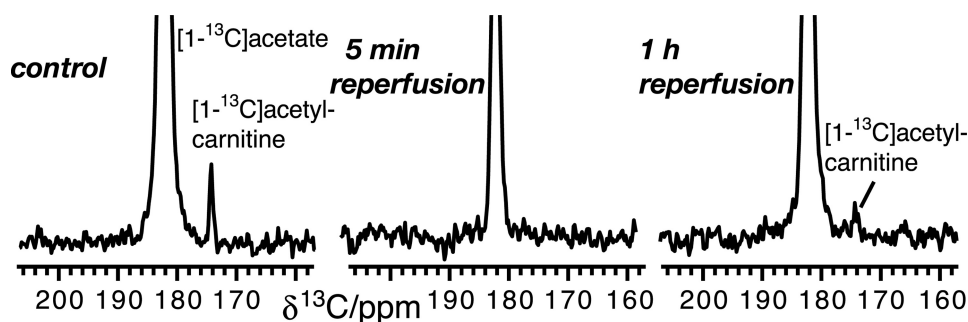


FIGURE 4. In vivo ^{13}C NMR spectra of acetate metabolism in skeletal muscle 5 min and 1 h after ischemia, as compared with control. Spectra were recorded as a time series (Fig. 3) and 8 traces recorded 4–32 s after the injection were summed. Acetate metabolism does not recover to preischemic values within 1 h.

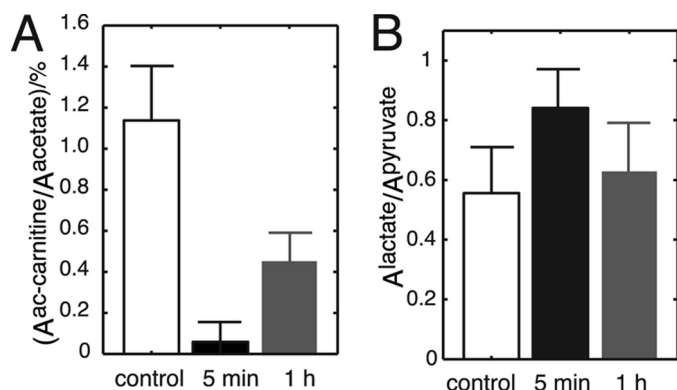


FIGURE 5. Formation of acetyl-carnitine is significantly reduced in ischemic mice, and disturbances of mitochondrial energy metabolism are easily detectable in vivo with hyperpolarized acetate for 1 h. Increased lactate fermentation is detectable in vivo with hyperpolarized $[1-^{13}\text{C}]$ pyruvate but is less persistent.

tate following ischemia. Most notably, the effect was pronounced both after 5 min and after 1 h of reperfusion (Fig. 4).

Statistical analysis of hyperpolarized $[1-^{13}\text{C}]$ acetate metabolism in mice shows that the ischemic group ($n = 3$) is significantly separate from the control group (Fig. 5A). Potential effects of altered tissue perfusion after ischemia were accounted for by relating $[1-^{13}\text{C}]$ acetyl-carnitine signal areas to $[1-^{13}\text{C}]$ acetate signal areas inside the muscle (Fig. 5A). This ratio is decreased from $1.14 \pm 0.26\%$ ($n = 3$) in the control group to $0.06 \pm 0.10\%$ ($n = 3$) in the second group with 5 min of reperfusion. After 1 h of reperfusion, the ratio is $0.42 \pm 0.16\%$ ($n = 3$) (Fig. 5A). Thus, the formation of acetyl-carnitine from exogenous $[1-^{13}\text{C}]$ acetate is reduced more than 10-fold right after the ischemic period ($p < 0.01$) and is still significantly decreased ($p < 0.02$) after 1 h of reperfusion.

Different Recovery of Different Pathways—Persistent metabolic changes in this ischemic model were subsequently assayed by alternative hyperpolarized substrates of mitochondrial and cytosolic reactions. Use of hyperpolarized $[1,4-^{13}\text{C}_2]$ fumarate was employed to assess TCA cycle activity with a substrate that is not reliant on co-substrates for conversion to its product malate. Formation of $[1,4-^{13}\text{C}_2]$ malate from $[1,4-^{13}\text{C}_2]$ fumarate is significantly increased from $0.74 \pm 0.19\%$ to $2.85 \pm 0.07\%$ ($p < 0.05$, $n = 2$) after 5 min and to $7.50 \pm 0.42\%$ ($p < 0.05$, $n = 2$) after 60 min of reperfusion. The increased formation of $[1,4-^{13}\text{C}_2]$ malate shows reduced rates of malate clearance relative to its synthesis, thus suggesting a reduced progression of subsequent reactions in the TCA cycle and overall reduced TCA cycle flux.

Hyperpolarized $[1-^{13}\text{C}]$ pyruvate as substrate for the cytosolic lactate dehydrogenase reaction on the other hand shows increased conversion to lactate upon ischemia. This is expected from increasing NADH:NAD⁺ ratios under hypoxic conditions (41). Pyruvate reduction to lactate is, however, significantly increased ($p < 0.01$) only shortly after ischemia has been released with an increase of the lactate:pyruvate ratio from 0.56 ± 0.15 (control; $n = 5$) to 0.84 ± 0.12 ($n = 5$), whereas deviations from control levels are insignificant ($p > 0.2$) after 1 h of reperfusion (lactate:pyruvate ratio 0.63 ± 0.15 ($n = 5$)) (Fig. 5B). This normalization in cytosolic pyruvate usage after

1 h is in contrast to abnormally low acetate metabolism by AceCS and CrAT as well as TCA cycle activity in mitochondria.

DISCUSSION

Acetate is a well-suited substrate for *in vivo* spectroscopy because of its fast cellular resorption and simple metabolism. Acetate supposedly is lipophilic enough to diffuse freely across membranes that separate subcellular compartments and thus sensitively reports on fluxes through AceCS- and CrAT-catalyzed reactions, even when this activity is sequestered in organelles.

Organ specific pathway activity of acetate metabolism as obtained in this study shows a larger flux of exogenous acetate to acetyl-carnitine in myocardium than in the liver. In the heart, the predominant AceCS2 isozyme activity implies uptake of exogenous acetate mostly into the mitochondrial acetyl-CoA pool and subsequent free equilibration with carnitine, thus allowing an increased flux of marker signal into the acetyl-carnitine pool. This is in principal agreement with the notion that fatty acids are major substrates of energy metabolism in myocardium (42) and that the mitochondrial isoforms AceCS2 predominates in the heart (1). In myocardium, skeletal muscle, and other tissues, AceCS2 supposedly functions to feed acetate into the TCA cycle as acetyl-CoA (43).

In liver, less acetyl-CoA flux to acetyl-carnitine is found than in the heart (Fig. 3). This reflects that the prevalence of different AceCS isoforms in both tissues results in organ-specific differences in acetate metabolism. In the liver, cytosolic AceCS1 provides acetyl-CoA for lipid synthesis. The putative absence both of mitochondrial AceCS2 and cytosolic CrAT supposedly avoids the use of acetate for acetyl-carnitine formation, mitochondrial import, and degradation in competition to lipogenesis (3, 34). The detection of acetyl-carnitine synthesis by *in vivo* DNP-NMR is thus surprising and indicates that fatty acid synthesis and oxidative metabolism compete for acetate in liver. The finding of acetyl-carnitine synthesis indicates either (i) the presence of non-negligible acetyl-CoA synthetase activity in liver peroxisomes, endoplasmic reticulum or mitochondria, (ii) presence of non-negligible CrAT activity in the cytosol, or (iii) specific uptake mechanisms of acetyl-CoA into cellular organelles (3). The possibility that acetyl-carnitine signal in liver results from synthesis outside the liver and subsequent resorption from plasma seems unlikely, as no significant increase in plasma levels of $[1-^{13}\text{C}]$ acetyl-carnitine was observed following injection of hyperpolarized $[1-^{13}\text{C}]$ acetate.

The capacity to detect tissue differences of hyperpolarized $[1-^{13}\text{C}]$ acetate metabolism *in vivo* allows the use of hyperpolarized $[1-^{13}\text{C}]$ acetate as noninvasive disease biomarker. Reduced acetate metabolism as observed by ^{13}C DNP-NMR *in vivo* up to 1 h after ischemia suggests that co-substrate pools (ATP, CoA, carnitine, see Fig. 2C) or enzyme activities for acetyl-carnitine synthesis from exogenous acetate are reduced following ischemia and normalize only slowly. Earlier studies suggest that ischemic muscle exhibits a cellular build-up of free fatty acids and their activated acyl-CoA and acyl-carnitine esters (8, 42, 44, 45). Free carnitine and CoA pools on the other hand decrease and get limiting to acetate metabolism, fatty acid oxidation, and pyruvate decarboxylation under conditions of low TCA cycle

flux in ischemia, acute myocardial infarction and cardiac failure (9, 17, 46–49).

Reduced pools of free carnitine and increased pools of acetyl-carnitine have previously been observed *ex vivo* after 30 min of recovery from anaerobic metabolism (48). ATP on the other hand retains preischemic levels because of buffering by phosphocreatine in the current ischemic model (36), while limited literature data on AceCS and CrAT expression give no indication of reduced enzyme levels under hypoxic conditions (50–52). Overall, this suggests that reduced, slowly recovering pools of free CoA and carnitine rather than ATP or enzyme levels are assayed by reduced acetate activation *in vivo* for more than 1 h after ischemia.

We find that acetate provides unique and sensitive information on cellular energy metabolism as compared with markers of glucose metabolism, because acetate metabolism is altered for a longer period of time after ischemia than *e.g.* pyruvate reduction (Fig. 5), which is affected by altered NADH and acetyl-CoA pools. The finding that acetate metabolism is more persistently affected by altered cosubstrate pools than pyruvate metabolism seems plausible in light of the high Michaelis-Menten constant K_m (0.4×10^{-3} M) of AceCS to CoA in cardiac muscle as compared with K_m values for CoA of 0.02×10^{-3} M for pyruvate dehydrogenase, 0.05×10^{-3} M for thiolase and 0.1×10^{-6} M for α -ketoglutarate dehydrogenase (17). This implies that CoA depletion following ischemia or high work loads will turn off AceCS activity faster than the other aforementioned CoA-dependent enzymes. Accordingly, AceCS activity is turned on later during recovery from CoA depletion than *e.g.* pyruvate dehydrogenase, thus suggesting the use of hyperpolarized $[1-^{13}\text{C}]$ acetate as a persistent marker of altered CoA and carnitine pools.

Free carnitine and CoA are indispensable for cellular energy metabolism and depend on the regeneration of CoA by the TCA cycle. We detect long-term alteration of TCA cycle flux upon ischemia-reperfusion in form of reduced clearance of malate by the cycle. Reduced flux of hyperpolarized $[1-^{13}\text{C}]$ pyruvate and $[2-^{13}\text{C}]$ pyruvate into the TCA cycle has been described in ischemic myocardium *in vivo* (25) and *ex vivo* (24, 33). The recovery of pyruvate dehydrogenase flux into the TCA cycle during reperfusion has however remained unclear, presumably because of the absence of long-chain fatty acids and ketones in *ex vivo* perfusion.

Reduced *in vivo* clearance of $[1,4-^{13}\text{C}_2]$ malate by the TCA cycle in ischemia-reperfusion in the current study directly shows that reaction fluxes in the cycle are reduced relative to the formation of malate by fumarase. Inhibition of TCA cycle enzymes α -ketoglutarate dehydrogenase, succinate dehydrogenase, and aconitase accordingly has been associated with the presence of reactive oxygen species when tissue is reoxygenated upon ischemia (53, 54), and enzymatic fluxes under oxidative stress await further studies *in vivo*. The submicromolar K_m of α -ketoglutarate dehydrogenase toward CoA suggests that TCA cycle activity in recovering skeletal muscle is not limited by CoA. Acetyl-CoA is unlikely to be limiting under conditions of increased beta oxidation following ischemia (55), especially as the K_m of citrate synthase toward acetyl-CoA (0.2 mM) indicates saturation (56, 57). Stable ATP levels (36) and fast recov-

ery of reduction equivalents as judged from recovering LDH flux in the current ischemia-reperfusion model thus indicate that altered fluxes in the TCA cycle result from inhibition of TCA cycle enzymes rather than limiting acetyl-CoA or cosubstrate pools. Overall, instantaneous measurements of acetate metabolism, TCA cycle, and anaerobic glycolysis *in vivo* demonstrate long lasting disturbance of mitochondrial bioenergetics following tissue hypoxia.

REFERENCES

1. Yamamoto, J., Ikeda, Y., Iguchi, H., Fujino, T., Tanaka, T., Asaba, H., Iwasaki, S., Ioka, R. X., Kaneko, I. W., Magoori, K., Takahashi, S., Mori, T., Sakaue, H., Kodama, T., Yanagisawa, M., Yamamoto, T. T., Ito, S., and Sakai, J. (2004) *J. Biol. Chem.* **279**, 16954–16962
2. Pouteau, E., Piloquet, H., Maugeais, P., Champ, M., Dumon, H., Nguyen, P., and Krempf, M. (1996) *Am. J. Physiol.* **271**, E58–E64
3. Ramsay, R. R., and Zammit, V. A. (2004) *Mol. Aspects Med.* **25**, 475–493
4. Rebouche, C. J., and Paulson, D. J. (1986) *Annu. Rev. Nutr.* **6**, 41–66
5. Bieber, L. L. (1988) *Annu. Rev. Biochem.* **57**, 261–283
6. Cordente, A. G., López-Viñas, E., Vázquez, M. I., Swiegers, J. H., Pretorius, I. S., Gómez-Puertas, P., Hegardt, F. G., Asins, G., and Serra, D. (2004) *J. Biol. Chem.* **279**, 33899–33908
7. Engel, A. G., and Angelini, C. (1973) *Science* **179**, 899–902
8. Bahl, J. J., and Bressler, R. (1987) *Annu. Rev. Pharmacol. Toxicol.* **27**, 257–277
9. Stephens, F. B., Constantin-Teodosiu, D., and Greenhaff, P. L. (2007) *J. Physiol.* **581**, 431–444
10. Hallows, W. C., Lee, S., and Denu, J. M. (2006) *Proc. Natl. Acad. Sci. U.S.A.* **103**, 10230–10235
11. North, B. J., and Sinclair, D. A. (2007) *Trends Biochem. Sci.* **32**, 1–4
12. Oyama, N., Akino, H., Kanamaru, H., Suzuki, Y., Muramoto, S., Yonekura, Y., Sadato, N., Yamamoto, K., and Okada, K. (2002) *J. Nucl. Med.* **43**, 181–186
13. Bertocci, L. A., Jones, J. G., Malloy, C. R., Victor, R. G., and Thomas, G. D. (1997) *J. Appl. Physiol.* **83**, 32–39
14. Gropler, R. J., Geltman, E. M., Sampathkumaran, K., Pérez, J. E., Schechtman, K. B., Conversano, A., Sobel, B. E., Bergmann, S. R., and Siegel, B. A. (1993) *J. Am. Coll. Cardiol.* **22**, 1587–1597
15. Malloy, C. R., Sherry, A. D., and Jeffrey, F. M. (1990) *Am. J. Physiol.* **259**, H987–H995
16. Brown, M., Marshall, D. R., Sobel, B. E., and Bergmann, S. R. (1987) *Circulation* **76**, 687–696
17. Robitaille, P. M., Rath, D. P., Abduljalil, A. M., O'Donnell, J. M., Jiang, Z., Zhang, H., and Hamlin, R. L. (1993) *J. Biol. Chem.* **268**, 26296–26301
18. Szczepaniak, L., Babcock, E. E., Malloy, C. R., and Sherry, A. D. (1996) *Magn. Reson. Med.* **36**, 451–457
19. Pouteau, E., Dumon, H., Bourge, V., Krempf, M., and Nguyen, P. (1998) *J. Nutr.* **128**, 2651S–2653S
20. Bertocci, L. A., and Lujan, B. F. (1999) *J. Appl. Physiol.* **86**, 2077–2089
21. Cerdan, S., Künnecke, B., and Seelig, J. (1990) *J. Biol. Chem.* **265**, 12916–12926
22. Malloy, C. R., Thompson, J. R., Jeffrey, F. M., and Sherry, A. D. (1990) *Biochemistry* **29**, 6756–6761
23. Ardenkjaer-Larsen, J. H., Fridlund, B., Gram, A., Hansson, G., Hansson, L., Lerche, M. H., Servin, R., Thaning, M., and Golman, K. (2003) *Proc. Natl. Acad. Sci. U.S.A.* **100**, 10158–10163
24. Merritt, M. E., Harrison, C., Storey, C., Sherry, A. D., and Malloy, C. R. (2008) *Magn. Reson. Med.* **60**, 1029–1036
25. Golman, K., Petersson, J. S., Magnusson, P., Johansson, E., Akeson, P., Chai, C. M., Hansson, G., and Månsson, S. (2008) *Magn. Reson. Med.* **59**, 1005–1013
26. Chen, A. P., Kurhanewicz, J., Bok, R., Xu, D., Joun, D., Zhang, V., Nelson, S. J., Hurd, R. E., and Vigneron, D. B. (2008) *Magn. Reson. Imaging* **26**, 721–726
27. Albers, M. J., Bok, R., Chen, A. P., Cunningham, C. H., Zierhut, M. L., Zhang, V. Y., Kohler, S. J., Tropp, J., Hurd, R. E., Yen, Y. F., Nelson, S. J., Vigneron, D. B., and Kurhanewicz, J. (2008) *Cancer Res.* **68**, 8607–8615
28. Chen, A. P., Albers, M. J., Cunningham, C. H., Kohler, S. J., Yen, Y. F., Hurd, R. E., Tropp, J., Bok, R., Pauly, J. M., Nelson, S. J., Kurhanewicz, J., and Vigneron, D. B. (2007) *Magn. Reson. Med.* **58**, 1099–1106
29. Golman, K., Zandt, R. L., Lerche, M., Pehrson, R., and Ardenkjaer-Larsen, J. H. (2006) *Cancer Res.* **66**, 10855–10860
30. Golman, K., in 't Zandt, R., and Thaning, M. (2006) *Proc. Natl. Acad. Sci. U.S.A.* **103**, 11270–11275
31. Day, S. E., Kettunen, M. I., Gallagher, F. A., Hu, D. E., Lerche, M., Wolber, J., Golman, K., Ardenkjaer-Larsen, J. H., and Brindle, K. M. (2007) *Nat. Med.* **13**, 1382–1387
32. Schroeder, M. A., Cochlin, L. E., Heather, L. C., Clarke, K., Radda, G. K., and Tyler, D. J. (2008) *Proc. Natl. Acad. Sci. U.S.A.* **105**, 12051–12056
33. Schroeder, M. A., Atherton, H. J., Ball, D. R., Cole, M. A., Heather, L. C., Griffin, J. L., Clarke, K., Radda, G. K., and Tyler, D. J. (2009) *Faseb J* **23**, 2529–2538
34. Zammit, V. A. (1999) *Prog. Lipid Res.* **38**, 199–224
35. Jensen, P. R., Meier, S., Ardenkjaer-Larsen, J. H., Duus, J. O., Karlsson, M., and Lerche, M. H. (2009) *Chem. Commun.* **34**, 5168–5170
36. in 't Zandt, H. J., Oerlemans, F., Wieringa, B., and Heerschap, A. (1999) *NMR Biomed.* **12**, 327–334
37. Naressi, A., Couturier, C., Devos, J. M., Janssen, M., Mangeat, C., de Beer, R., and Graveron-Demilly, D. (2001) *Magma* **12**, 141–152
38. Fujino, T., Kondo, J., Ishikawa, M., Morikawa, K., and Yamamoto, T. T. (2001) *J. Biol. Chem.* **276**, 11420–11426
39. Bloisi, W., Colombo, I., Garavaglia, B., Giardini, R., Finocchiaro, G., and Didonato, S. (1990) *Eur. J. Biochem.* **189**, 539–546
40. Farrell, S. O., Fiol, C. J., Reddy, J. K., and Bieber, L. L. (1984) *J. Biol. Chem.* **259**, 13089–13095
41. Kobayashi, K., and Neely, J. R. (1983) *J. Mol. Cell Cardiol.* **15**, 359–367
42. Whitmer, J. T., Idell-Wenger, J. A., Rovetto, M. J., and Neely, J. R. (1978) *J. Biol. Chem.* **253**, 4305–4309
43. Wolfe, A. J. (2005) *Microbiol. Mol. Biol. Rev.* **69**, 12–50
44. Idell-Wenger, J. A., Grotyohann, L. W., and Neely, J. R. (1978) *J. Biol. Chem.* **253**, 4310–4318
45. Calvani, M., Reda, E., and Arrigoni-Martelli, E. (2000) *Basic Res. Cardiol.* **95**, 75–83
46. Iliceto, S., Scutrinio, D., Bruzzi, P., D'Ambrosio, G., Boni, L., Di Biase, M., Biasco, G., Hugenholtz, P. G., and Rizzon, P. (1995) *J. Am. Coll. Cardiol.* **26**, 380–387
47. Shug, A. L., Thomsen, J. H., Folts, J. D., Bittar, N., Klein, M. I., Koke, J. R., and Huth, P. J. (1978) *Arch. Biochem. Biophys.* **187**, 25–33
48. Minkler, P. E., Brass, E. P., Hiatt, W. R., Ingalls, S. T., and Hoppel, C. L. (1995) *Anal. Biochem.* **231**, 315–322
49. Kobayashi, A., and Fujisawa, S. (1994) *J. Mol. Cell Cardiol.* **26**, 499–508
50. Aharinejad, S., Schäfer, R., Hofbauer, R., Abraham, D., Blumer, R., Mikovsky, A., Traxler, H., Pullirsch, D., Alexandrowicz, R., Taghavi, S., Kocher, A., and Laufer, G. (2001) *Transplantation* **72**, 1043–1049
51. Yoshii, Y., Furukawa, T., Yoshii, H., Mori, T., Kiyono, Y., Waki, A., Kobayashi, M., Tsujikawa, T., Kudo, T., Okazawa, H., Yonekura, Y., and Fujibayashi, Y. (2009) *Cancer Sci.* **100**, 821–827
52. Hülsmann, W. C., and Dubelaar, M. L. (1992) *Mol. Cell Biochem.* **116**, 125–129
53. Nulton-Persson, A. C., and Szwedra, L. I. (2001) *J. Biol. Chem.* **276**, 23357–23361
54. Hoerter, J., Gonzalez-Barroso, M. D., Couplan, E., Mateo, P., Gelly, C., Cassard-Doulier, A. M., Diolez, P., and Bouillaud, F. (2004) *Circulation* **110**, 528–533
55. Kudo, N., Barr, A. J., Barr, R. L., Desai, S., and Lopaschuk, G. D. (1995) *J. Biol. Chem.* **270**, 17513–17520
56. Shepherd, D., and Garland, P. B. (1969) *Biochem. J.* **114**, 597–610
57. Leonardi, R., Zhang, Y. M., Rock, C. O., and Jackowski, S. (2005) *Prog. Lipid Res.* **44**, 125–153